

## S-Nitrosylation of NF- $\kappa$ B p65 Inhibits TSH-Induced Na<sup>+</sup>/I<sup>-</sup> Symporter Expression

Juan Pablo Nicola,\* Victoria Peyret,\* Magalí Nazar, Jorge Miguel Romero, Ariel Maximiliano Lucero, María del Mar Montesinos, José Luis Bocco, Claudia Gabriela Pellizas, and Ana María Masini-Repiso

Centro de Investigaciones en Bioquímica Clínica e Inmunología (J.P.N., V.P., M.N., A.M.L., M.d.M.M., J.L.B., C.G.P., A.M.M.-R.) and Centro de Investigaciones en Química Biológica (J.M.R.), Consejo Nacional de Investigaciones Científicas y Técnicas, Facultad de Ciencias Químicas, Universidad Nacional de Córdoba, Córdoba, Argentina

Nitric oxide (NO) is a ubiquitous signaling molecule involved in a wide variety of cellular physiological processes. In thyroid cells, NO-synthase III-endogenously produced NO reduces TSH-stimulated thyroid-specific gene expression, suggesting a potential autocrine role of NO in modulating thyroid function. Further studies indicate that NO induces thyroid dedifferentiation, because NO donors repress TSH-stimulated iodide (I<sup>-</sup>) uptake. Here, we investigated the molecular mechanism underlying the NO-inhibited Na<sup>+</sup>/I<sup>-</sup> symporter (NIS)-mediated I<sup>-</sup> uptake in thyroid cells. We showed that NO donors reduce I<sup>-</sup> uptake in a concentration-dependent manner, which correlates with decreased NIS protein expression. NO-reduced I<sup>-</sup> uptake results from transcriptional repression of NIS gene rather than posttranslational modifications reducing functional NIS expression at the plasma membrane. We observed that NO donors repress TSH-induced NIS gene expression by reducing the transcriptional activity of the nuclear factor- $\kappa$ B subunit p65. NO-promoted p65 S-nitrosylation reduces p65-mediated transactivation of the NIS promoter in response to TSH stimulation. Overall, our data are consistent with the notion that NO plays a role as an inhibitory signal to counterbalance TSH-stimulated nuclear factor- $\kappa$ B activation, thus modulating thyroid hormone biosynthesis. (*Endocrinology* 156: 0000–0000, 2015)

Iodide (I<sup>-</sup>) plays a key role in thyroid physiology as an essential component of the thyroid hormones and as a regulator of thyroid function (1, 2). Na<sup>+</sup>/I<sup>-</sup> symporter (NIS)-mediated I<sup>-</sup> uptake across the basolateral plasma membrane of thyrocytes constitutes the first step in thyroid hormone biosynthesis (2). TSH is the main regulator of I<sup>-</sup> uptake and NIS expression in thyroid cells. TSH-induced cAMP production stimulates I<sup>-</sup> transport by increasing NIS gene transcription (3, 4). The regulatory region controlling rat NIS gene expression contains a proximal promoter between nucleotides –110 and –420 relative to the transcription start site, and a strong TSH-

responsive far-upstream enhancer (NIS upstream enhancer [NUE]) between nucleotides –2264 and –2495 (4). The NUE region contains 2 thyroid transcription factor 1-binding sites that have no apparent effect on NIS transcription, 2 paired box 8 (Pax8)-binding sites, and a degenerate cAMP-response element. Full TSH-dependent NIS gene transcription requires at least 1 Pax8-binding site and the integrity of the cAMP-response element sequence (5). We have previously described the role of the nuclear factor (NF)- $\kappa$ B subunit p65 in the regulation of NIS gene transcription through direct interaction with an NF- $\kappa$ B-binding site within the NUE region (6). In addition, the

ISSN Print 0013-7227 ISSN Online 1945-7170  
Printed in USA  
Copyright © 2015 by the Endocrine Society  
Received February 27, 2015. Accepted July 22, 2015.

\* J.P.N. and V.P. contributed equally to this work.

Abbreviations: ChIP, chromatin immunoprecipitation; cGK, cGMP-dependent protein kinase; cGMP, cyclic GMP; cPTIO, 2-(4-carboxyphenyl)-4,4,5,5-tetramethylimidazole-1-oxyl-3-oxide; dbcAMP, dibutyryl-cAMP; FRTL-5, Fisher rat thyroid cell line 5; FSK, forskolin; GSNO, S-nitrosoglutathione; HA, hemagglutinin; I<sup>-</sup>, iodide;  $\kappa$ B, NF- $\kappa$ B inhibitor; NF- $\kappa$ B, nuclear factor- $\kappa$ B; NIS, Na<sup>+</sup>/I<sup>-</sup> symporter; NO, nitric oxide; NOS, NO synthase; NUE, NIS upstream enhancer; Pax8, paired box 8; qPCR, quantitative PCR; SDS, sodium dodecyl sulfate; SNP, sodium nitroprusside; SPNO, spermine NONOate; TPO, thyroid peroxidase; TSHR, TSH receptor

transcription factor p65 functionally cooperates with Pax8 in the regulation of NIS gene expression (6).

Nitric oxide (NO) is a ubiquitous signaling molecule involved in a wide variety of physiological processes. However, chronic overproduction of NO is associated with various cancerous and autoimmune diseases (7, 8). Endogenous NO is generated from L-arginine by NO synthase (NOS). The members of the NOS family, named NOS I–III, are widely expressed. In particular, NOS III is abundantly expressed in the thyroid follicular cells (9, 10), and basal levels of endogenous NO-induced cyclic guanosine monophosphate ~~cyclic GMP~~ (cGMP) production have been reported (11). Gérard et al (12) demonstrated that NOS III expression is restricted to active thyroid follicles, suggesting a paracrine role for NO in the modulation of microvascular blood flow. Moreover, NO donors have been reported to inhibit I<sup>-</sup> uptake and organification in various thyroid cell models (13–15). We have previously investigated the role of endogenous NO production in thyroid cell function and differentiation using nonselective NOS inhibitors, and concluded that endogenous NO acts as a negative regulator of TSH-stimulated gene expression and proliferation in thyrocytes (16). Together, these results suggest that NO participates in an inhibitory autocrine feedback loop in the regulation of TSH-dependent thyroid cell function.

The best characterized physiological mediator of NO action, known as the canonical signaling pathway, is the soluble guanylate cyclase. NO activates soluble guanylate cyclase to produce the secondary messenger cGMP, thus activating cGMP-dependent protein kinases (cGKs) (17). In addition, a noncanonical, cGMP-independent NO signaling pathway involves the posttranslational S-nitrosylation of specific cysteine residues to regulate protein structure and activity (17) ~~(the process commonly known as S-nitrosylation is also called nitrosation; the latter term is more chemically accurate)~~. Compelling evidence suggests that NO regulates gene expression by modulating the transcriptional activity of many transcription factors through S-nitrosylation (18). Indeed, S-nitrosylation is the primary molecular mechanism by which NO modulates NF- $\kappa$ B signaling (19). S-nitrosylation regulates the ~~NF- $\kappa$ B regulatory kinase IKK- $\beta$~~  and the transcriptionally active NF- $\kappa$ B subunits p50 and p65. In particular, S-nitrosylation of p65 at ~~Cys-38~~ inhibits p65 DNA binding and p65-dependent gene transcription (20).

Various studies have demonstrated that the classical NO donor sodium nitroprusside (SNP) down-regulates TSH-induced I<sup>-</sup> uptake in thyroid cells (13–15). Accordingly, inhibition of NOS activity, resulting in suppression of NO production, increases TSH-stimulated I<sup>-</sup> uptake (16). Therefore, investigation of the molecular mechanism

by which NO regulates I<sup>-</sup> uptake could provide critical information regarding the role of NO in modulating TSH-induced thyroid hormonogenesis. Thus, we have examined the mechanism involved in the NO-induced inhibition of NIS-mediated I<sup>-</sup> uptake in thyroid cells. Here, we provide evidence supporting the notion that NO-modulated NIS gene transcriptional expression involves S-nitrosylation of the NF- $\kappa$ B subunit p65, which reduces transactivation of the NIS promoter in response to TSH stimulation.

## Materials and Methods

### Plasmids

The -2854 to +13-bp DNA fragment (pNIS-2.8) of the rat NIS promoter and the NIS enhancer region (NUE)-deleted construct (pNIS-2.0) were as described (21). The -2495 to -2264-bp DNA fragment of the far-upstream enhancer NUE cloned 5' upstream to the thymidine kinase promoter (pNUE) and its site-directed mutants were as reported (5, 6). The NF- $\kappa$ B reporter vector containing 5  $\kappa$ B consensus sites linked to the luciferase coding sequence (pNF- $\kappa$ B-Luc) was obtained from Clontech. The Pax8 reporter gene (5xPax8-Luc) and the cAMP-responsive gene (5xCRE-Luc) were as described (22, 23). The normalization reporter pCMV- $\beta$ -galactosidase was purchased from Promega. Expression vectors encoding amino-terminal hemagglutinin (HA)-tagged wild-type NIS (HA-NIS), flag-tagged wild-type p65, and flag-tagged C38S p65 were as reported (24–26).

### Important note

### Cell culture

The thyroid cell line Fisher rat thyroid cell line 5 (FRTL-5) (ATCC CRL-1468) was cultured in DMEM/Ham F-12 medium supplemented with 5% calf serum (Life Technologies), 1-mIU/mL bovine TSH (National Hormone and Peptide Program), 10- $\mu$ g/mL bovine insulin, and 5- $\mu$ g/mL bovine transferrin (Sigma-Aldrich) (27). FRTL-5 cells stably expressing HA-NIS were selected and propagated in growth media containing 300- $\mu$ g/mL G418 (Sigma-Aldrich). When cells reached 50%–60% confluence, they were cultured in the same media except without TSH and containing only 0.2% calf serum (basal media) for 5 days before treatment. TSH-starved cells were treated with different concentrations of ~~SNP~~ (Calbiochem), S-nitrosoglutathione (GSNO) (Sigma-Aldrich), or spermine NONOate (SPNO) (Sigma-Aldrich) in the absence or presence of 0.5-mIU/mL TSH for the indicated periods of time. The NO scavenger 2-(4-carboxyphenyl)-4,4,5,5-tetramethylimidazole-1-oxyl-3-oxide (cPTIO) (Sigma-Aldrich) was used in an amount equimolar to the concentration of NO donors. After treatments, cell viability was higher than 95%, as determined by the Trypan blue dye exclusion assay (see Supplemental Materials and Methods).

### I<sup>-</sup> uptake

Cells were incubated in modified Hanks' balanced salt solution (10mM HEPES [pH 7.5], 140mM NaCl, 5.4mM KCl, 1.3mM CaCl<sub>2</sub>, 0.4mM MgSO<sub>4</sub>, 0.5mM MgCl<sub>2</sub>, 0.4mM Na<sub>2</sub>HPO<sub>4</sub>, 0.44mM KH<sub>2</sub>PO<sub>4</sub>, and 5.6mM glucose) containing

AQ: 11

AQ: 12

AQ: 13

AQ: 14

AQ: 7

AQ: 8

AQ: 9

AQ: 10

20  $\mu$ M NaI supplemented with 10  $\mu$ Ci/ $\mu$ mol  $I^-$  carrier-free  $Na^{125}I$  (PerkinElmer Life and Analytical Sciences) for 30 minutes at 37°C (28). Accumulated radioiodide was extracted with 95% ice-cold ethanol and then quantified in a  $\gamma$ -counter (Beckman Gamma 4000, Beckman Coulter). The DNA amount was determined by the diphenylamine method on the nonethanol extracted material after trichloroacetic acid precipitation.  $I^-$  uptake was expressed as pmol  $I^-/\mu$ g DNA.

### Cell surface biotinylation

FRTL-5 cells were incubated with 0.5-mg/mL sulfo-NH-SS-biotin (Pierce Biotechnology) in 20mM HEPES (pH 8.5), 2mM  $CaCl_2$ , and 150mM NaCl for 15 minutes at 4°C. Excess of sulfo-NH-SS-biotin was quenched with PBS containing 100mM glycine. Cells were lysed in 50mM Tris-HCl (pH 7.5), 150mM NaCl, 5mM EDTA, 1% Triton X-100, 0.1% sodium dodecyl sulfate (SDS) at 4°C for 20 minutes. 100  $\mu$ g protein was incubated overnight at 4°C with streptavidin agarose beads (Pierce Biotechnology). Beads were washed and adsorbed proteins were eluted with sample buffer at 75°C for 5 minutes and analyzed by immunoblotting as described below.

### Flow cytometry

Paraformaldehyde-fixed cells were incubated in PBS containing 0.2% BSA for nonpermeabilized conditions or an additional 0.2% saponin for permeabilized conditions with 1:800 rabbit monoclonal anti-HA antibody (Cell Signaling), followed by 0.4- $\mu$ g/mL Alexa Fluor 488-conjugated goat antirabbit antibody (Molecular Probes). The fluorescence of  $2 \times 10^4$  cells per experimental sample was assayed in FACS Canto II flow cytometer (BD Biosciences). All data were analyzed with FlowJo software (Tree Star).

### Immunoblotting

For total protein extracts, FRTL-5 cells were resuspended in whole-cell lysate buffer (50mM HEPES [pH 7], 2mM  $MgCl_2$ , 250mM NaCl, 0.1mM EDTA, 0.1mM EGTA, 0.1% Nonidet P-40) supplemented with protease inhibitors, and incubated on ice for 15 minutes (29). Cytoplasmic and nuclear protein fractionation was performed using ProteoJET extraction kit (Fermentas Life Sciences). Polypeptides were resolved by SDS-PAGE and electrotransferred to nitrocellulose membranes (Whatman). Information regarding primary antibodies is presented in Table 1. Proteins were visualized by the enhanced chemiluminescence Western blotting detection system (Pierce Biotechnology). Band intensities were measured densitometrically using ImageJ Software (National Institutes of Health).

### Real-time PCR

Total RNA purification, cDNA synthesis, and quantitative PCR (qPCR) were performed as described (30). Gene-specific primer sets were as follow: NIS (270 bp), 5'-GCTGTGGCAT TGTCATGTTTC (forward) and 5'-TGAGGTCTCCACAGT CACA (reverse); Pax8 (256 bp), 5'- CAGTTGTCGACTGAG CATCG (forward) and 5'- GCGTCCCAGAGGTGTATTGG (reverse); NF- $\kappa$ B inhibitor ( $I\kappa$ B)- $\alpha$  (217 bp), 5'-CCGAGACTT TCGAGGAAATACC (forward) and 5'-GAGCGTTGACATC AGCACC (reverse); and  $\beta$ -actin (138 bp), 5'-GGCACCAC ACTTTCTACAATG (forward) and 5'-TGGCTGGGGTG TTGAAGGT (reverse). Relative changes in gene expression were calculated using the  $2^{-\Delta\Delta C_t}$  method normalized against the housekeeping gene  $\beta$ -actin. Primers used for chromatin immunoprecipitation (ChIP) analysis were as reported (6). For each pair of primers a dissociation plot resulted in a single peak, indicating that only 1 cDNA species was amplified. Specific target amplification was confirmed by automatic sequencing (Macrogen). qPCR efficiency for each pair of primers was calculated

**Table 1.** Antibody Table

| Peptide/ Protein Target | Antigen Sequence                           | Name of Antibody        | Manufacturer, Catalog Number, and/or Name of Individual Providing the Antibody | Species Raised in; Monoclonal or Polyclonal | Dilution Used                  |
|-------------------------|--|-------------------------|--|---|--------------------------------|
| NIS p65                 | Proprietary<br>C terminus of human p65     | —<br>C-20               | Dr Nancy Carrasco<br>sc-372G, Santa Cruz<br>Biotechnology, Inc                 | Rabbit; Polyclonal<br>Goat; polyclonal      | 0.4 $\mu$ g/mL<br>2 $\mu$ g/mL |
| Pax8                    | C terminus of human Pax8                   | PAX8R1                  | sc-81353, Santa Cruz<br>Biotechnology, Inc                                     | Mouse; monoclonal                           | 2 $\mu$ g/mL                   |
| $I\kappa$ B- $\alpha$   | Full-length human $I\kappa$ B- $\alpha$    | H-4                     | sc-1643, Santa Cruz<br>Biotechnology, Inc                                      | Mouse; monoclonal                           | 4 $\mu$ g/mL                   |
| TSHR                    | Amino acids 1–155 of human TSHR            | H-155                   | sc-13936, Santa Cruz<br>Biotechnology, Inc                                     | Rabbit; polyclonal                          | 1 $\mu$ g/mL                   |
| TPO                     | TPO purified from human thyroid microsomes | MoAb47                  | sc-58432, Santa Cruz<br>Biotechnology, Inc                                     | Mouse; monoclonal                           | 8 $\mu$ g/mL                   |
| Histone H1              | Unknown                                    | AE-4                    | sc-8030, Santa Cruz<br>Biotechnology, Inc                                      | Mouse; monoclonal                           | 1 $\mu$ g/mL                   |
| HA-Tag                  | YPYDVPDYA                                  | C29F4                   | 3724, Cell Signaling   | Rabbit; monoclonal                          | 1:1000                         |
| Flag-Tag                | DYKDDDDK                                   | —                       | F7425, Sigma-Aldrich   | Rabbit; polyclonal                          | 1 $\mu$ g/mL                   |
| $\beta$ -Actin          | DDDIAALVIDDGSYGK                           | AC-15                   | A1978, Sigma-Aldrich   | Mouse; monoclonal                           | 0.5 $\mu$ g/mL                 |
| $\alpha$ -Tubulin       | Unknown                                    | B-5-1-2                 | T5168, Sigma-Aldrich   | Mouse; monoclonal                           | 0.2 $\mu$ g/mL                 |
| E-cadherin              | Amino acids 735–883 of human E-cadherin    | Clone 36/<br>E-cadherin | 610181, BD Transduction<br>Laboratories  | Mouse; monoclonal                           | 0.25 $\mu$ g/mL                |

T1

AQ: 15

AQ: 28

using standard curves generated by serial dilutions of cDNA or genomic DNA of FRTL-5 cells. All qPCR efficiencies ranged between 97%–105% in different assays.

### Transient transfection and reporter gene assay

FRTL-5 cells were transiently transfected with 2  $\mu$ g of luciferase reporter-promoter constructs per well in 6-well plates using Lipofectamine 2000 (Life Technologies). To study promoter activity, cells were split into 24-well plates at 80% confluence the day after transfection. The next day, growth media was replaced with basal media and transfected cells were starved and treated as stated above. The luciferase activity was measured using a Luciferase Assay System (Promega) according to manufacturer's instructions. To assess transfection efficiency, cells were cotransfected with 0.2  $\mu$ g/well of the normalization reporter  $\beta$ -galactosidase. Luciferase activities were normalized relative to  $\beta$ -galactosidase activity values.

When the effect of C38S p65 was tested, FRTL-5 cells were cotransfected with luciferase reporter-promoter constructs (0.9  $\mu$ g), p65 expression vectors (2.6  $\mu$ g), and  $\beta$ -galactosidase reporter vector (0.1  $\mu$ g) per well of a 6-well plate.

### Biotin-switch assay for S-nitrosylation

The biotin switch assay was performed in virtual darkness as previously described (31). In brief, FRTL-5 cells were disrupted by gentle sonication in HEN buffer (100mM HEPES [pH 7.8], 1mM EDTA, and 0.1mM neocuproine). Typically, 600  $\mu$ g of total proteins were incubated in blocking buffer (2.5% SDS and 20mM N-ethylmaleimide in HEN buffer) to block-free thiol groups. After removing excess N-ethylmaleimide by acetone precipitation, nitrosothiols were reduced to thiols with 3mM ascorbic acid. The newly formed thiols were then linked to the sulfhydryl-specific biotinylating reagent N-[6-(biotinamido)hexyl]-3'-(2'-pyridyldithio) propionamide (Pierce Biotechnology). After removing excess N-[6-(biotinamido)hexyl]-3'-(2'-pyridyldithio) propionamide by acetone precipitation, biotinylated proteins were diluted to 1 mg/mL in neutralization buffer (20mM HEPES [pH 7.7], 100mM NaCl, 1mM EDTA, 0.1% SDS, and 0.5% Triton X-100) and pulled down using neutralization buffer-equilibrated streptavidin-agarose beads (Sigma-Aldrich). The resin was washed 5 times with neutralization buffer containing 600mM NaCl, twice with neutralization buffer containing 1M NaCl and once with regular neutralization buffer. Bound-proteins were eluted in Laemmli sample buffer containing 1% 2-mercaptoethanol and Western blot analysis to detect the S-nitrosylated proteins was performed as described above.

### Chromatin immunoprecipitation

ChIP assays were performed as previously described (29). Briefly, cells were cross-linked in culture media containing 1% formaldehyde. Nuclei were purified and lysed in 50mM Tris-HCl (pH 8), 10mM EDTA, and 1% SDS. Genomic DNA was broken by sonication and 10-fold diluted in IP dilution buffer (50mM Tris-HCl [pH 7.5], 150mM NaCl, 5mM EDTA, 1% Triton X-100, and 0.5% Nonidet P-40). Immunoprecipitation was performed with 2  $\mu$ g of affinity-purified monoclonal anti-p65 antibody (sc-8008; Santa Cruz Biotechnology, Inc) or control mouse IgG. Immune complexes were purified with Protein A/G PLUS-Agarose (Santa Cruz Biotechnology, Inc). Immuno-

precipitates were washed 4 times with IP dilution buffer containing 0.1% SDS; twice with high-salt IP wash buffer (50mM Tris-HCl [pH 7.5], 500mM NaCl, 5mM EDTA, 0.1% SDS, and 1% Triton X-100), and once with ~~TE buffer (10mM Tris-HCl [pH 8] and 1mM EDTA)~~. DNA was purified using Chelex-100 (Bio-Rad). Immunoprecipitated DNA was quantified by qPCR as mentioned above. Relative fold increase was calculated according to the equation:  $2^{-[Ct.input - Ct.target] - (Ct.input - Ct.mock)}$ .

### Statistical analysis

Results are reported as the mean  $\pm$  SD. One-way ANOVA with Newman-Keuls multiple comparisons post hoc test was performed using GraphPad Prism (GraphPad Software) from at least 3 independent experiments. Differences were considered statistically significant at  $P < .05$ .

## Results

### NO donors inhibit TSH-induced I<sup>-</sup> uptake

Previous studies have shown that NO donors inhibit TSH-stimulated I<sup>-</sup> uptake in various thyroid cell models (13–15). Therefore, to understand the molecular mechanism involved in NO-inhibited I<sup>-</sup> uptake, we first determined the effect of different NO donors on TSH-induced I<sup>-</sup> uptake in FRTL-5 thyroid cells. Thyroid cells were treated with different concentrations of one of 3 structurally unrelated NO donors, SNP, GSNO, or SPNO, in the presence of TSH (0.5 mIU/mL) for 24 hours. As previously reported (13, 14), treatment of thyroid cells with SNP (50  $\mu$ M–500  $\mu$ M) inhibited TSH-stimulated I<sup>-</sup> uptake in a concentration-dependent manner (Figure 1A). A similar inhibitory effect was observed with the physiologically relevant nitrosothiol GSNO (200  $\mu$ M) and the NO-releasing agent SPNO (100  $\mu$ M), which yields approximately physiological steady-state concentrations of NO (Figure 1B). Perchlorate (ClO<sub>4</sub><sup>-</sup>), a competitive NIS inhibitor, reduced I<sup>-</sup> accumulation to levels comparable with those of TSH-starved cells, suggesting NIS-mediated I<sup>-</sup> accumulation (Supplemental Figure 1A). In addition, no NO donors tested had a significant effect on I<sup>-</sup> uptake in TSH-starved cells (Supplemental Figure 1B). Nor was any significant effect of NO donors observed on TSH-stimulated I<sup>-</sup> uptake in the presence of the cell-permeating NO scavenger cPTIO (Figure 1B). Moreover, TSH-induced I<sup>-</sup> uptake was slightly higher when endogenously generated NO was sequestered by cPTIO (Figure 1B) (16).

To analyze the mechanism underlying NO donor-inhibited I<sup>-</sup> uptake, FRTL-5 cells were treated with TSH in the presence or absence of NO donors, and NIS protein expression at the plasma membrane was assessed using cell surface biotinylation assays. As previously reported (32), TSH stimulation increased NIS expression at the plasma membrane (Figure 1C). However, NO donors re-

AQ: 17

F1

AQ: 16

Important note

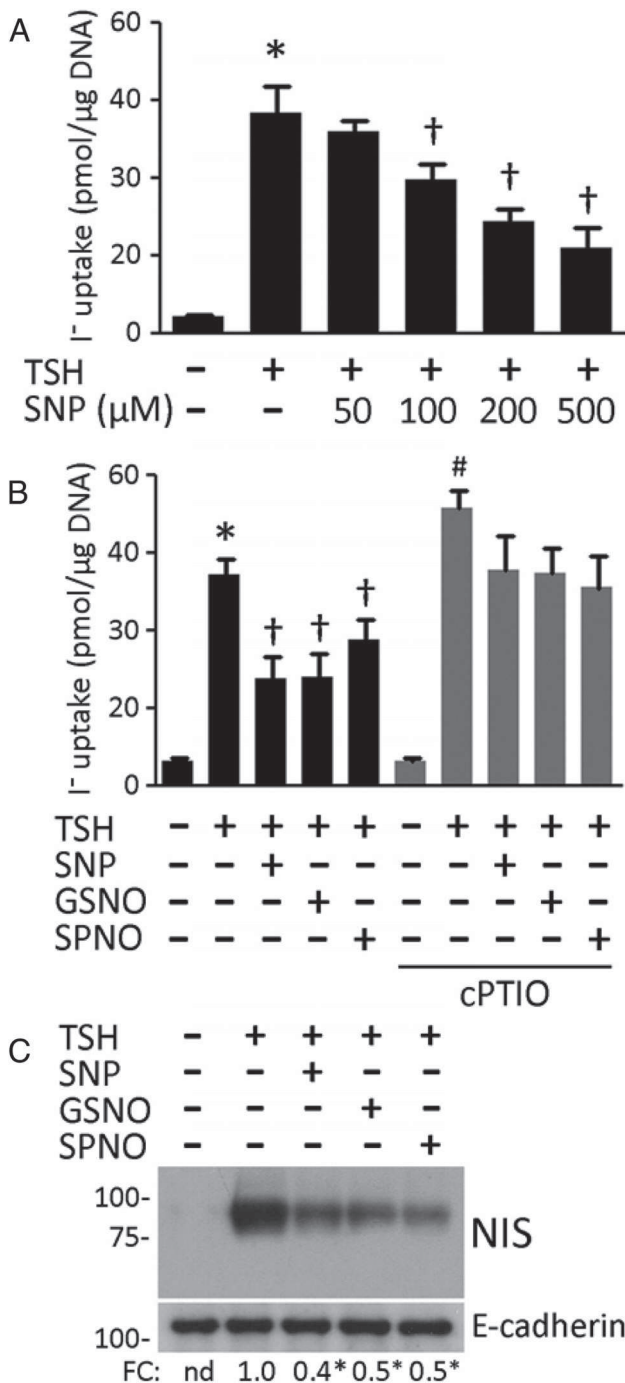


**Figure 1.** NO donors inhibit TSH-induced I<sup>-</sup> uptake. A, I<sup>-</sup> uptake in FRTL-5 cells stimulated with 0.5-mIU/mL TSH in the presence or absence of 50 μM–500 μM SNP for 24 hours. I<sup>-</sup> uptake results are expressed as pmol I<sup>-</sup>/μg DNA. \*, P < .05 vs basal condition; †, P < .05 vs TSH-treated cells. B, I<sup>-</sup> uptake in FRTL-5 cells incubated with 0.5-mIU/mL TSH in the presence or absence of 200 μM SNP or GSNO, and 100 μM SPNO for 24 hours. The NO scavenger cPTIO (200 μM) was incubated with the media containing the NO donors for 30 minutes before addition to the cells. \*, P < .05 vs basal condition; †, P < .05 vs TSH-treated cells; #, P < .05 vs TSH treated in the absence of cPTIO. C, Representative cell surface biotinylation assay measuring NIS expression at the plasma membrane in FRTL-5 cells stimulated with 0.5-mIU/mL TSH in the presence or absence of the indicated NO donors for 24 hours. Immunoblot analysis only revealed an approximately 80-kDa plasma membrane-located fully glycosylated NIS

duced TSH-induced cell surface NIS levels (Figure 1C). Considering that functional NIS expression at the plasma membrane accounts for I<sup>-</sup> accumulation, these results provide a potential explanation for the reduction of NIS-mediated I<sup>-</sup> uptake in the presence of NO donors: NO donors either impair the trafficking of NIS to the plasma membrane or, alternatively, reduce the biosynthesis of NIS protein.

### NO donors do not modulate NIS expression at the posttranscriptional level

To determine whether NO donors repress the targeting of NIS to the plasma membrane, we engineered FRTL-5 cells stably expressing wild-type NIS containing a HA epitope at the extracellular amino terminus (HA-NIS), whose expression is controlled by a constitutive non-TSH-regulated promoter. This system allows us to determine the amount of NIS at the cell surface using an anti-HA antibody under nonpermeabilized conditions. To determine the functionality and intracellular distribution of the fusion protein, Cos-7 cells were transiently transfected with vectors encoding wild-type NIS or HA-NIS. I<sup>-</sup> uptake assays showed that HA tagging does not affect NIS function (Supplemental Figure 2A), suggesting that the HA epitope does not affect targeting of NIS to the plasma membrane. This was further confirmed by confocal microscopy (Supplemental Figure 2B). To determine the NO donor-induced posttranslational mechanisms affecting NIS function or cell surface expression, HA-NIS-expressing FRTL-5 cells were cultured without TSH to down-regulate their endogenous NIS expression and further incubated with NO donors for 24 hours. I<sup>-</sup> uptake assays demonstrated that NO donors do not significantly affect the activity of the exogenous NIS fusion protein (Figure 2A). Immunoblot analysis using an anti-HA antibody demonstrated constitutive expression of the fusion protein despite the presence of TSH (Figure 2B). TPO expression was measured to assess TSH responsiveness (Figure 2B). Flow cytometry under nonpermeabilized conditions using an anti-HA antibody demonstrated that NO donors did not modify cell surface HA-NIS expression in FRTL-5 cells (Figure 2C, surface). Moreover, flow cytometry assessing HA-NIS expression under permeabilized conditions indicated that NO donors did not modulate total HA-NIS expression (Figure 2C, total). Taken together, these findings indicate that the decrease in I<sup>-</sup> uptake

**Figure 1. (Continued).** polypeptide. Expression of the plasma membrane protein E-cadherin was used as a loading control. Undetectable α-tubulin staining indicated the absence of cytoplasmic protein contamination (data not shown). Fold change (FC) represents the mean of results from 3 independent experiments. nd, not detectable. \*, P < .05 vs TSH-treated cells.

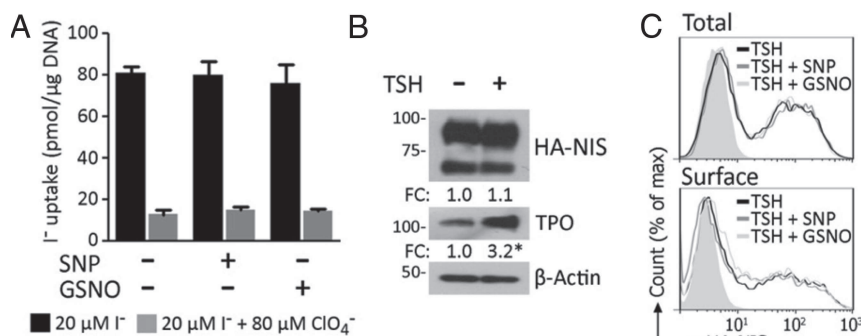


**Figure 2.** NO donors do not modulate NIS expression at the posttranscriptional level. A, I<sup>-</sup> uptake in TSH-starved FRTL-5 cells stably expressing HA-NIS incubated with 200 μM SNP or GSNO for 24 hours. I<sup>-</sup> transport assays were performed in the absence or presence of the NIS competitive inhibitor perchlorate (ClO<sub>4</sub><sup>-</sup>). Results are expressed as pmol I<sup>-</sup>/μg DNA. B, Representative immunoblot assessing HA expression in FRTL-5 cells permanently expressing HA-NIS. TSH-starved cells were stimulated with 0.5-mIU/mL TSH for 24 hours. TPO expression was used to evaluate TSH responsiveness, and β-actin was used as a loading control. Fold change (FC) represents the mean of results from at least 3 independent experiments. C, Representative histograms showing total NIS expression (total) and NIS expression at the plasma membrane (surface) quantified by flow cytometry using an anti-HA antibody. HA-NIS-expressing FRTL-5 cells were incubated with 200 μM NO donor in the presence of 0.5-mIU/mL TSH for 24 hours. Geometric mean ± SD of results from 3 independent experiments: TSH, 128 ± 12; TSH + SNP, 118 ± 8; TSH + GSNO, 122 ± 6 (total); TSH, 137 ± 14; TSH + SNP, 133 ± 18; and TSH + GSNO, 132 ± 15 (surface). Data from negative controls without the primary antibody are shown in solid grey histograms.

caused by NO donors is not due to internalization of NIS molecules from the plasma membrane or to posttranslational modifications affecting NIS activity or stability.

### NO donors inhibit forskolin (FSK) and cAMP-stimulated I<sup>-</sup> uptake

In thyroid cells, TSH stimulates I<sup>-</sup> uptake through a cAMP-mediated increase in NIS gene expression. Activation of the cAMP pathway by FSK, an adenylyl cyclase activator, or by cAMP analogs mimics TSH-induced I<sup>-</sup> uptake (3, 33). Therefore, we analyzed the effect of NO donors on FSK- or dibutyl-rl-cAMP (dbcAMP)-stimulated I<sup>-</sup> uptake in FRTL-5 cells. Consistent with previous findings (33), FSK and dbcAMP treatment induced I<sup>-</sup> uptake. In addition, SNP and GSNO reduced FSK- and dbcAMP-increased I<sup>-</sup> uptake (Figure 3A), suggesting that the effect of NO occurs downstream of TSH receptor (TSHR) activation and cAMP synthesis. Supporting these observations, Bazzara et al (13) reported that SNP concentrations below 500 μM did not significantly affect TSH-triggered cAMP production in rat thyrocytes.

We further investigated TSHR protein expression in response to NO donors. Treatment of FRTL-5 cells with SNP or GSNO did not significantly modify TSHR protein expression (Figure 3B), ruling out the possibility that changes in TSHR expression mediate the effect of NO donors on TSH-stimulated I<sup>-</sup> uptake. Moreover, we examined changes in the activity of the cAMP-responsive vector 5xCRE-Luc under TSH stimulation in the presence

of NO donors for 24 hours. In FRTL-5 cells transiently transfected with 5xCRE-Luc, neither SNP nor GSNO significantly affected the activity of the TSH-induced cAMP-responsive vector (Figure 3C), indicating that NO donors did not modulate the CRE-dependent cAMP-induced transcriptional effect. Specificity in the response of 5xCRE-Luc to TSH stimulation was measured in the presence of the PKA inhibitor H89 (Figure 3C). Complementarily, we determined the effect of NO donors on the reporter activity of 5xCRE-Luc upon stimulation with either FSK or dbcAMP. NO donors did not regulate FSK- or dbcAMP-stimulated cAMP-responsive vector activity (Supplemental Figure 3), supporting the notion that the effect of NO occurs independently of the activation by the PKA-dependent cAMP signaling pathway of the transcription factor cAMP-response element-binding protein.

AQ:18,19

### NO donors inhibit TSH-stimulated NIS transcriptional expression

A decrease in I<sup>-</sup> transport may be the result of different mechanisms, such as blockage of NIS activity, a decrease in NIS expression at the plasma membrane, or a decrease in NIS protein biogenesis. Therefore, because NO donors reduced I<sup>-</sup> uptake in thyroid cells (Figure 1, A and B) independently of posttranslational modifications (Figure 2), we investigated whether NO donors modulate TSH-stimulated NIS protein expression. We observed that treatment with SNP (50 μM–500 μM) for 24 hours significantly reduced TSH-stimulated NIS protein expression in a concentration-dependent manner (Figure 4A). Consistent with this, we observed that the NO donors GSNO and SPNO significantly reduced TSH-stimulated NIS protein expression (Figure 4B). Interestingly, our data suggest that NO donors repress NIS-mediated I<sup>-</sup> uptake by reducing NIS protein biogenesis, causing fewer NIS molecules to reach the plasma membrane.

To investigate the mechanism involved in NO-reduced NIS protein expression, we measured TSH-stimulated NIS mRNA expression in the presence of various NO donors. Incubation of FRTL-5 cells with SNP, GSNO, or SPNO for 24 hours led to NIS mRNA levels significantly lower than those observed in control cells (Figure 4C), suggest-

F4

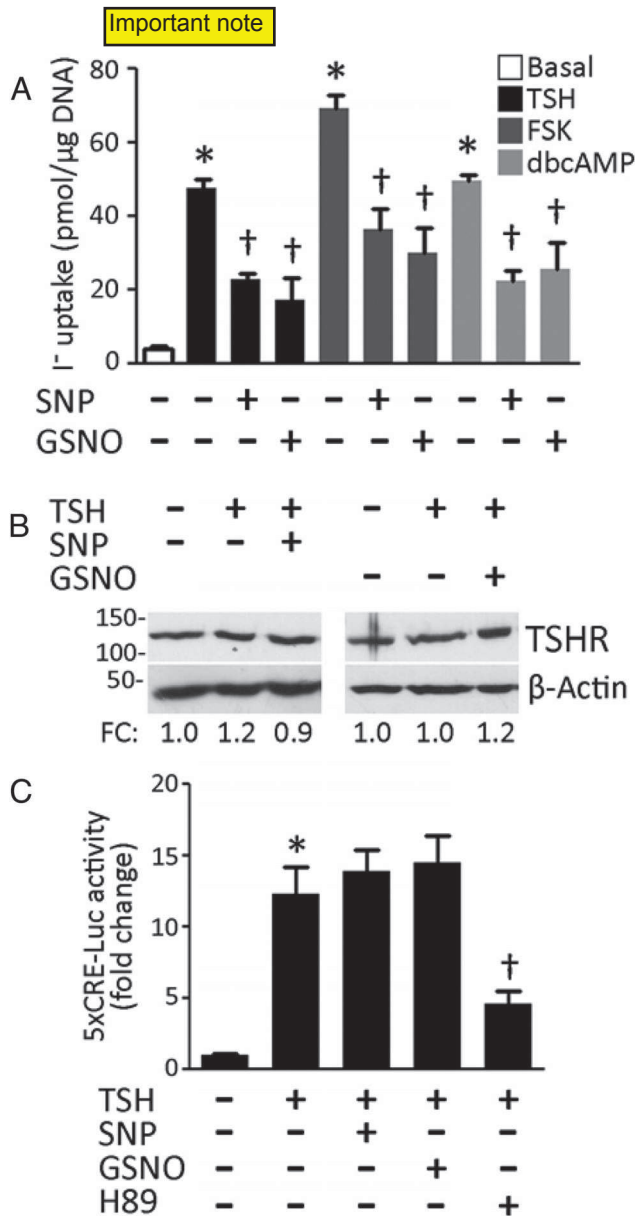


**Figure 3.** NO donors do not inhibit the cAMP signaling pathway activating the transcription factor cAMP-response element-binding protein (CREB). A, I<sup>-</sup> uptake in FRTL-5 cells stimulated with 0.5-mIU/mL TSH, 10μM FSK, or 0.5mM dbcAMP in the presence or absence of 200μM NO donor for 24 hours. Results are expressed as pmol I<sup>-</sup>/μg DNA. \*, *P* < .05 vs basal condition; †, *P* < .05 vs TSH-, FSK-, or dbcAMP-treated cells. B, Representative immunoblot analysis of TSHR protein expression in FRTL-5 cells treated with 200μM NO donor in the presence of 0.5-mIU/mL TSH for 24 hours. β-Actin was used as a loading control. Fold change (FC) represents the mean of results from at least 3 independent experiments. C, Relative activity of the cAMP-responsive vector 5xCRE-Luc in response to 200μM SNP or GSNO in the presence of 0.5-mIU/mL TSH for 24 hours. The PKA inhibitor H89 (10μM) was added 30 minutes before TSH stimulation. \*, *P* < .05 vs basal condition; †, *P* < .05 vs TSH-treated cells.

ing that NO-reduced TSH-stimulated NIS expression involves transcriptional repression of the NIS gene.

Complementarily, to investigate NO-induced NIS gene transcriptional repression, we assessed the effect of NO donors on the NIS gene regulatory sequence. FRTL-5 cells

transfected with the luciferase reporter construct pNIS-2.8 were treated with SNP or GSNO (200μM) in the presence of TSH for 24 hours. Consistent with previous findings (21), TSH stimulated pNIS-2.8 reporter activity, whereas NO donors induced significant repression of TSH-induced NIS transcriptional activation (Figure 4D). We further investigated the NIS gene regulatory region responsible for NO-induced NIS down-regulation by analyzing the transcriptional activity of a 5'-deleted NIS reporter construct missing the NUE region (pNIS-2.0). In accordance with previous findings (4), the far-upstream enhancer NUE was required for full TSH stimulation of NIS gene transcriptional activation, whereas NO donors had no effect on the transcriptional activity of the NIS reporter construct pNIS-2.0 (Figure 4D). These findings suggest that NO represses TSH-dependent transcriptional activation of the NIS gene by a mechanism involving *cis*-elements within the NUE region.

### NO donors do not modulate Pax8 transcriptional activity

The transcription factor Pax8 is involved in maintaining thyroid differentiation, and is essential for the expression of thyroid differentiation markers required for thyroid hormone biosynthesis (34). In particular, Pax8 expression is essential for NIS gene expression. The far-upstream enhancer NUE contains 2 functionally relevant Pax8-binding sites surrounding a central cAMP-response element-like element (5). Therefore, we assessed the effect of NO donors on Pax8 protein expression in response to TSH treatment. Neither SNP (50μM–200μM) nor GSNO (200μM) modulates TSH-up-regulated Pax8 protein expression (Figure 5, A and B). In accordance, NO donors did not significantly affect Pax8 mRNA levels (Figure 5C). Subsequently, we tested the effect of NO donors on Pax8 transcriptional activity in response to TSH stimulation using a construct driving the expression of luciferase under the control of Pax8 (5xPax8-Luc). None of the tested NO donors significantly reduced TSH-stimulated Pax8-dependent transcriptional activity (Figure 5D).

Complementarily, we investigated the effect of NO donors on a TSH-responsive NIS enhancer region (NUE) construct lacking Pax8-binding sites. FRTL-5 cells were transfected with the indicated NUE mutant constructs linked to the thymidine kinase promoter and treated with 200μM NO donors in the presence of TSH for 24 hours. Consistent with the findings indicating that NO donors repress NIS gene transcription by a mechanism involving *cis*-elements within the NUE region (Figure 4D), we observed that NO donors significantly repressed TSH-stimulated pNUE reporter activity (Figure 5E). Interestingly, mutagenesis at 2 Pax8-binding sites (Pax8-A and Pax8-C)

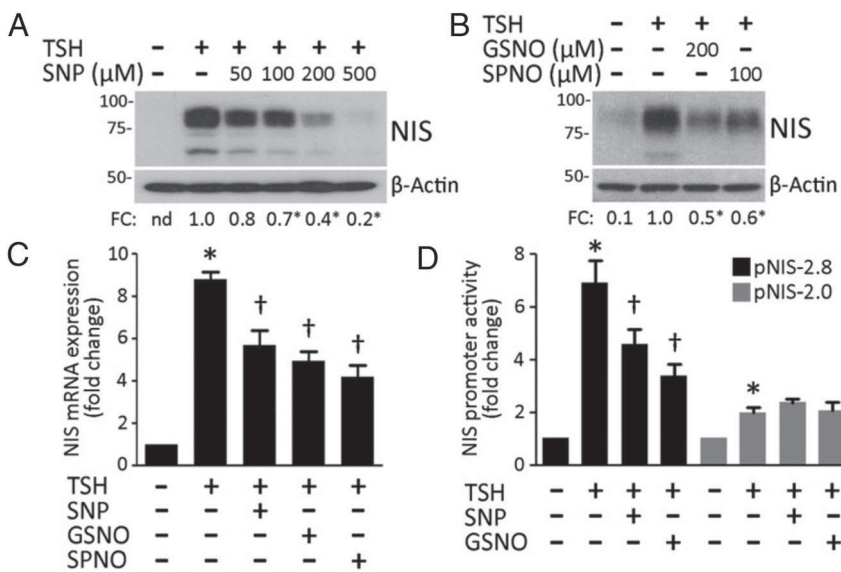


**Figure 4.** NO donors inhibit TSH-stimulated NIS transcriptional expression. A and B, Representative immunoblot analysis of NIS protein expression in FRTL-5 cells stimulated with 0.5-mIU/mL TSH in the presence of NO donors at the indicated concentrations for 24 hours. The NIS electrophoretic pattern showed an approximately 80-kDa fully glycosylated and an approximately 55-kDa partially glycosylated polypeptide.  $\beta$ -Actin was used as a loading control. Densitometric analysis was performed to determine the relative expression of fully glycosylated NIS normalized to  $\beta$ -actin. Fold change (FC) represents the mean of results from at least 3 independent experiments. nd, not detectable. \*,  $P < .05$  vs TSH-treated cells. C, Relative NIS mRNA expression assessed by RT/qPCR. Cells were stimulated with 200  $\mu$ M SNP or GSNO, or 100  $\mu$ M SPNO, in the presence of 0.5-mIU/mL TSH for 24 hours. Results are shown as FC relative to the mRNA levels of untreated cells. \*,  $P < .05$  vs basal condition; †,  $P < .05$  vs TSH-treated cells. D, FRTL-5 cells were transiently transfected with the indicated NIS promoter constructs linked to luciferase. Starved cells were treated with 200  $\mu$ M NO donor in the presence of 0.5-mIU/mL TSH for 24 hours. Results are expressed as luciferase activity normalized to that of  $\beta$ -galactosidase and relative to basal activity for each construct. \*,  $P < .05$  vs basal condition; †,  $P < .05$  vs TSH-treated cells.

resulted in dissimilar responses to NO donors. Although both reporters respond significantly to TSH stimulation, NO donors repressed pNUE-A activity, whereas disruption of Pax8-binding site C (pNUE-C) impaired NO responsiveness (Figure 5E). By contrast, the NIS enhancer construct lacking both Pax8-binding sites (pNUE-AC) is mostly insensitive to TSH stimulation (Figure 5E) (4). Hence, although Pax8-binding site C (NUE-C) modulates the transcriptional activity of the NUE enhancer in response to NO donors, Pax8 transcriptional activity is not affected by NO donors (Figure 5D), suggesting that binding of Pax8 to Pax8-binding site C is required for NO to modulate NIS gene expression. Consistent with this notion, we have previously described a functional interaction complex composed of Pax8 and the NF- $\kappa$ B-subunit p65 that synergistically regulates NIS transcriptional expression in response to external stimulus (6).

### NO donors repress p65-dependent NIS expression

Given that the NF- $\kappa$ B p65 subunit induces NIS gene expression, and the importance of binding of Pax8 to the *cis*-regulatory element Pax8-C to functionally synergize with p65, which binds to the NUE-C-adjacent  $\kappa$ B-binding

site (6), we further investigated whether NO suppresses TSH-dependent NIS gene expression by repressing TSH-induced NF- $\kappa$ B signaling.

Induction of NF- $\kappa$ B signaling in FRTL-5 cells after TSHR activation has been reported previously (35, 36). Under basal conditions, transcriptionally active NF- $\kappa$ B subunits are sequestered in the cytoplasm as inactive complexes bound to members of the I $\kappa$ B family (37). In the canonical pathway, NF- $\kappa$ B-activating agents induce the phosphorylation and subsequent proteasomal degradation of I $\kappa$ B proteins, causing NF- $\kappa$ B subunits to enter the nucleus and regulate gene transcription (38). Using immunoblotting, we studied 2 hallmarks of NF- $\kappa$ B signaling activation, I $\kappa$ B- $\alpha$  degradation and nuclear accumulation of p65, in FRTL-5 cells treated with TSH in the presence of NO donors for 1 hour. We observed I $\kappa$ B- $\alpha$  degradation (Figure 6A) and nuclear accumulation of p65 (Figure 6B) in response to TSH treatment; coinubation with NO donors significantly affected neither I $\kappa$ B- $\alpha$  degradation nor p65 nuclear

recruitment, suggesting that NO does not repress TSH-activated NF- $\kappa$ B signaling. We subsequently tested the ability of NO donors to regulate TSH-induced NF- $\kappa$ B-dependent gene expression in thyroid cells using an artificial NF- $\kappa$ B reporter (pNF- $\kappa$ B-Luc). FRTL-5 cells transfected with the luciferase reporter pNF- $\kappa$ B-Luc were incubated with NO donors in the presence of TSH for 24 hours. We observed that TSH-induced pNF- $\kappa$ B-Luc reporter activity was significantly reduced in the presence of NO donors, suggesting that NO represses TSH-induced NF- $\kappa$ B-dependent gene transcription (Figure 6C). Assay specificity was tested in the presence of the NF- $\kappa$ B-specific inhibitor BAY 11-7082 (Figure 6C).

NF- $\kappa$ B activity is modulated by negative regulators that are themselves highly regulated NF- $\kappa$ B targets. In particular, I $\kappa$ B proteins are among the earliest NF- $\kappa$ B-induced targets that play an important role in terminating NF- $\kappa$ B response (39). Therefore, we measured I $\kappa$ B- $\alpha$  mRNA expression to determine whether NO donors repress TSH-induced NF- $\kappa$ B transcriptional activity. As expected, we observed a significant increase in I $\kappa$ B- $\alpha$  mRNA expression in response to treatment with TSH for 24 hours (Figure 6D).

F6

AQ: 20



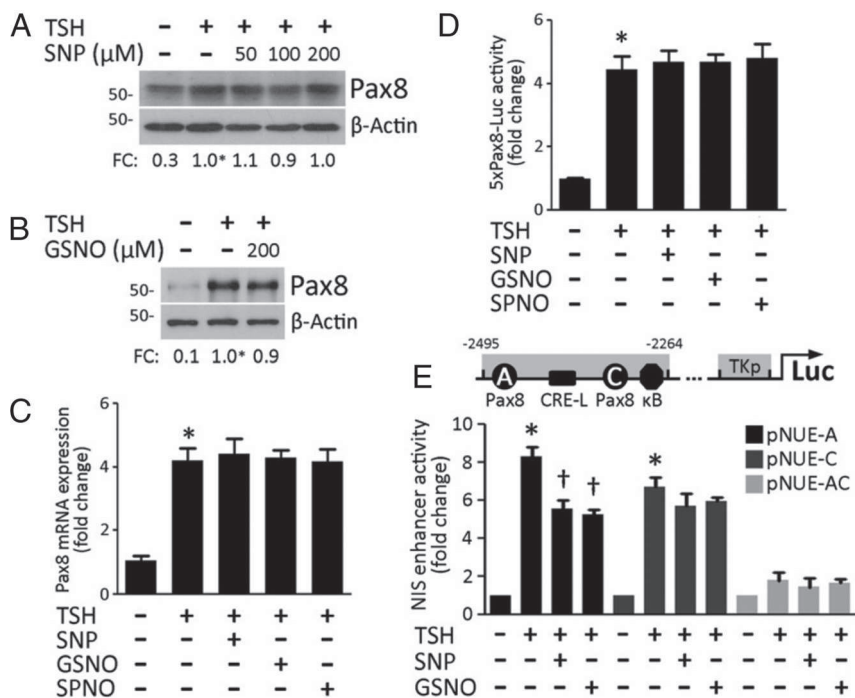


**Figure 5.** NO donors do not modulate Pax8 transcriptional activity. A and B, Representative immunoblot analysis of Pax8 protein expression in FRTL-5 cells stimulated with 50μM–500μM SNP or 200μM GSNO in the presence of 0.5-mIU/mL TSH for 24 hours. β-Actin expression was used as a loading control. Fold change (FC) represents the mean of results from at least 3 independent experiments. \*, *P* < .05 vs nontreated cells. C, Relative Pax8 mRNA expression levels in cells stimulated with 200μM SNP or GSNO, or 100μM SPNO, in the presence of 0.5-mIU/mL TSH for 24 hours. Results are given as FC relative to the mRNA levels of untreated cells. \*, *P* < .05 vs basal condition. D, Relative activity levels of the Pax8 reporter 5xPax8-Luc in response to 200μM SNP or GSNO, or 100μM SPNO, in the presence of 0.5-mIU/mL TSH for 24 hours. \*, *P* < .05 vs basal condition. E, upper panel, Schematic representation of the ~~–2495 to –2264 (bp) DNA~~ fragment of the far-upstream enhancer NUE cloned 5'-upstream of the thymidine kinase promoter (TKp). Shapes represent the indicated transcription factor-binding sites. Lower panel, Cells were transiently transfected with the indicated Pax8-binding site missing NIS enhancer constructs linked to luciferase and treated with 200μM NO donor in the presence of 0.5-mIU/mL TSH for 24 hours. Results are expressed as luciferase activity normalized to that of β-galactosidase and relative to basal activity for each construct. \*, *P* < .05 vs basal condition; †, *P* < .05 vs TSH-treated cells.

Consistent with the NO-repressed pNF-κB-Luc reporter activity, TSH-induced IκB-α mRNA expression was significantly reduced in NO donor-treated cells (Figure 6D).

We further investigated the role of NF-κB as a potential target of NO-induced NIS transcriptional repression. FRTL-5 cells were transfected with a pNUE reporter whose κB-binding site was disrupted by site-directed mutagenesis (pNUE-κB MT) and subjected to treatment with NO donors in the presence of TSH for 24 hours. Interestingly, although disruption of the κB-binding site reduced TSH-induced NIS promoter activity (6), it rendered NO donors completely unable to repress TSH-induced NIS enhancer activity (Figure 6E).

We further examined the binding of NF-κB subunit p65 to the NIS promoter using ChIP assays. In line with previous findings (6), quantitative ChIP analysis revealed p65 enrichment in sequences spanning the κB site within the

NUE region in response to treatment with TSH for 1 hour (Figure 6F). Moreover, NO donor treatment significantly reduced the TSH-induced binding of p65 to the NIS promoter. In the control experiment, p65 enrichment in the immunoprecipitates was consistently reduced in the presence of BAY 11–7082 (Figure 6F). Therefore, these results indicate that NO decreased TSH-stimulated NIS transcriptional expression by impairing the binding of the NF-κB subunit p65 to the NIS promoter.

### NO donor-induced p65 S-nitrosylation inhibits NIS transcriptional expression

NO-induced p65 S-nitrosylation is a posttranscriptional mechanism important for regulating the binding of p65 to DNA and thus inhibiting p65-mediated gene expression (20). Therefore, considering that NO donors inhibited the recruitment of p65 to the NUE, we investigated the role of S-nitrosylation of p65 at Cys-38 in NO-repressed NIS expression. FRTL-5 cells were cotransfected with the reporter pNUE along with an expression vector encoding p65 in which Cys-38 was replaced with the nonnitrosylatable residue serine (C38S) or with wild-type p65 as a control. After starvation, cells were treated with NO donors in the

presence of TSH for 24 hours. Interestingly, impairment of Cys-38 S-nitrosylation prevented NO-induced NIS transcriptional repression (Figure 7A). Importantly, using a similar experimental approach, we demonstrated that C38S p65 does not affect TSH-induced NF-κB-dependent reporter activity (Figure 7B). Immunoblot analysis demonstrated equal p65 protein expression in wild-type and C38S p65-transfected cells (Figure 7C). Overall, these data suggest that NO-mediated posttranscriptional modification of p65 at Cys-38 constitutes an essential step in repressing p65-dependent NIS transcriptional expression.

To determine whether NO-induced p65 transcriptional repression is mediated by S-nitrosylation, we evaluated the presence of S-nitrosylated p65 in cell lysates generated from FRTL-5 cells treated with different NO donors in the presence of TSH for 1 hour. Using biotin switch assays

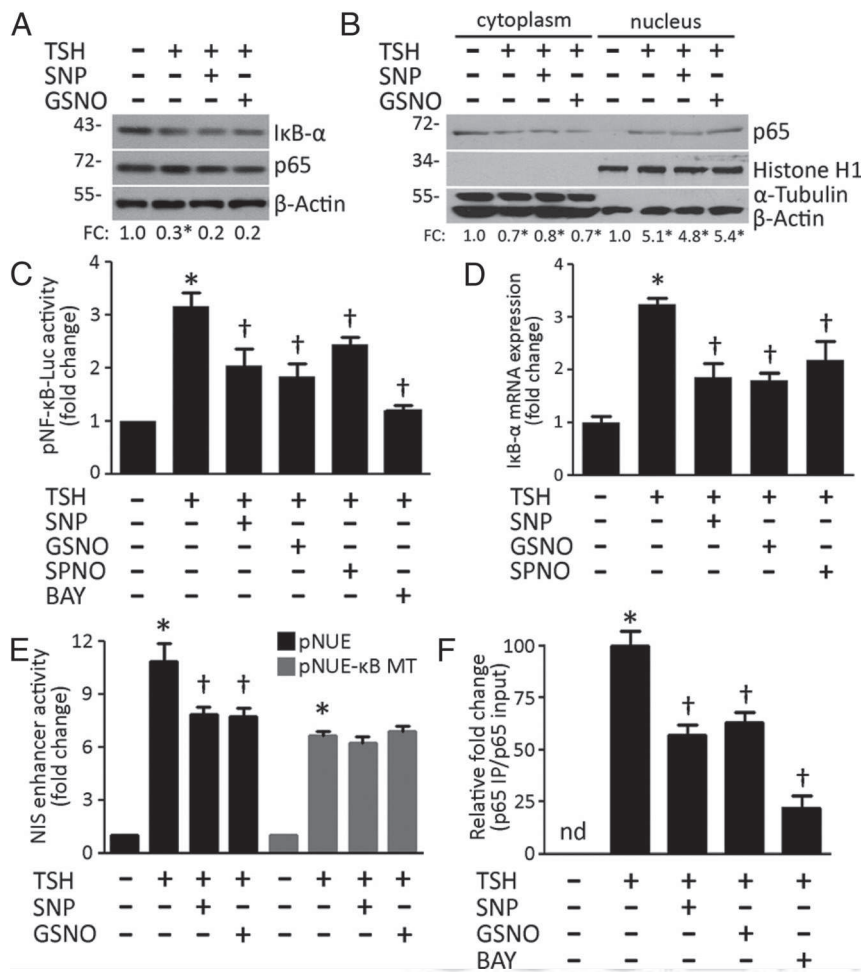


**Figure 6.** NO donors inhibit TSH-induced NF-κB transcriptional activity. A, Representative immunoblot analysis showing IκB-α and p65 protein levels in response to 200 μM NO donor in the presence of 0.5-mIU/mL TSH for 1 hour. β-Actin expression was used as a loading control. Fold change (FC) represents the mean of results from at least 3 independent experiments. \*, *P* < .05 vs basal condition. B, Representative immunoblot analysis of p65 nuclear recruitment in response to 200 μM NO donor in the presence of 0.5-mIU/mL TSH for 1 hour. Staining of the cytoplasmic marker α-tubulin or the nuclear marker histone H1 served to establish the separation of nuclear from cytoplasmic fractions. β-Actin expression was used as a loading control. FC represents the mean of results from at least 3 independent experiments. \*, *P* < .05 vs basal condition. C, Relative activity of the NF-κB reporter vector pNF-κB-Luc in response to 200 μM SNP or GSNO, or 100 μM SPNO, in the presence of 0.5-mIU/mL TSH for 24 hours. The IκB BAY 11-7082 (1 μM) was added 30 minutes before TSH stimulation. \*, *P* < .05 vs basal condition; †, *P* < .05 vs TSH-treated cells. D, Relative IκB-α mRNA expression in cells stimulated with 200 μM SNP or GSNO, or 100 μM SPNO, in the presence of 0.5-mIU/mL TSH for 24 hours. Results are given as FC relative to the mRNA levels of untreated cells. \*, *P* < .05 vs basal condition; †, *P* < .05 vs TSH-treated cells. E, Cells were transiently transfected with the indicated NIS enhancer constructs linked to luciferase and treated with 200 μM NO donor in the presence of 0.5-mIU/mL TSH for 24 hours. Results are expressed as luciferase activity normalized to that of β-galactosidase and relative to basal activity for each construct. \*, *P* < .05 vs basal condition; †, *P* < .05 vs TSH-treated cells. F, Starved cells were treated with 200 μM NO donor in the presence of 0.5-mIU/mL TSH for 1 hour before cross-linking and a further ChIP assay. The IκB BAY 11-7082 (1 μM) was added 30 minutes before TSH stimulation. Results are expressed as relative fold increase (p65 IP/p65 input). nd, not detectable. \*, *P* < .05 vs basal condition; †, *P* < .05 vs TSH-treated cells.

(40), p65 S-nitrosylation was detectable in response to the nitrosylation agent GSNO, unlike control and TSH-treated cells (Figure 7D). We further established that p65 S-nitrosylation was not affected only by the nitrosylating

agent GSNO, because SNP- and SPNO-treated cells also showed detectable p65 S-nitrosylation (Figure 7D). Taken together, our data demonstrate that NO-induced p65 S-nitrosylation modulates TSH-dependent NIS transcriptional expression (Figure 7E).

## Discussion

Thyroid function is strictly regulated by TSH, although other factors, such as intrathyroidal I<sup>-</sup> levels and thyroid follicle-stored thyroglobulin, function as autocrine negative feedback regulators of thyroid hormone biosynthesis. Endogenous TSH-induced NO production has been implicated in the regulation of the thyroid function, because NO signaling controls several events in thyroid hormonogenesis (16). Previous observations have indicated that NO donors inhibit I<sup>-</sup> uptake in different thyroid cell models. Kasai et al (41) and Costamagna et al (14) described a regulatory role for NO as an inhibitor of I<sup>-</sup> organification in primary cultures of human and bovine thyroid follicles. Consistent with this, NOSH<sup>-/-</sup> produced NO partially mediates proinflammatory-cytokine-repressed thyroid peroxidase (TPO) and thyroid oxidase expression in human thyrocytes (42, 43). More recently, Bazzara et al (13) have reported that NO donors inhibit TSH-induced TPO and thyroglobulin mRNA expression in rat thyroid cells.

Thyroid microvasculature is key for sustaining thyroid function, and thyrocytes play a critical role in its regulation. In particular, NO may participate in controlling thyroid vascularity and blood flow during thyroid dysfunction. Colin et al (10) reported abundant NOS III expression in thyroid cells during goitrogenesis, because animals treated with the NOS inhibitor N-nitro-L-arginine methyl ester showed a 36%

reported abundant NOS III expression in thyroid cells during goitrogenesis, because animals treated with the NOS inhibitor N-nitro-L-arginine methyl ester showed a 36%

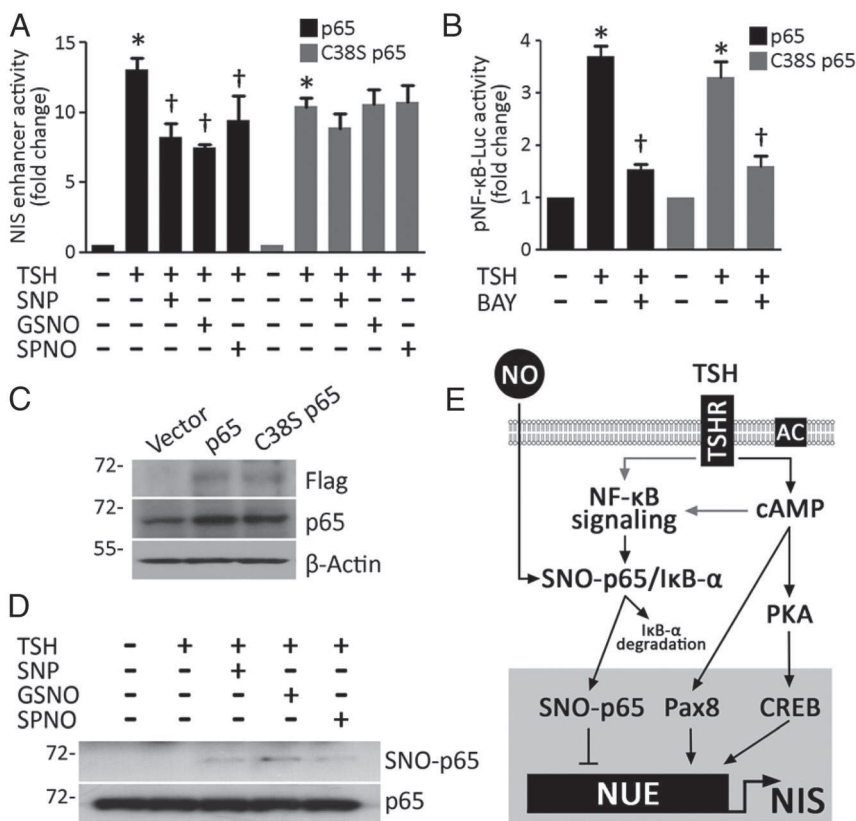


**Figure 7.** p65 S-nitrosylation mediates NO donor-induced NIS transcriptional repression. A, FRTL-5 cells were cotransfected with the reporter pNUE along with the expression vector encoding wild-type or C38S p65. After starvation, cells were treated with 200 μM SNP or GSNO, or 100 μM SPNO, in the presence of 0.5-mIU/mL TSH for 24 hours. Results are expressed as luciferase activity normalized to that of β-galactosidase and relative to pNUE basal activity. \*, *P* < .05 vs basal condition; †, *P* < .05 vs TSH-treated cells. B, Relative activity levels of the NF-κB-dependent reporter pNF-κB-Luc in response to TSH (0.5 mIU/mL) treatment for 24 hours in FRTL-5 cells overexpressing wild-type or C38S p65. Results are expressed as luciferase activity normalized to that of β-galactosidase and relative to pNF-κB-Luc basal activity. BAY 11-7082 (1 μM) was used as a specificity control. \*, *P* < .05 vs basal condition; †, *P* < .05 vs TSH-treated cells. C, Representative immunoblot analysis of whole-protein extracts obtained from FRTL-5 cells transiently transfected with wild-type or C38S p65. Exogenously overexpressed wild-type and C38S p65 were detected with anti-FLAG and anti-p65 antibodies. Loading was assessed by β-actin expression. D, Biotin-switch assay showing p65 S-nitrosylation in response to 200 μM SNP or GSNO, and 100 μM SPNO, in the presence of 0.5-mIU/mL TSH for 1 hour. Undetectable p65 S-nitrosylation was observed in untreated and TSH-treated cells. p65 immunoblots are shown for both the S-nitrosylated protein (SNO-p65) and the input lysate (p65). E, Summary schematic representation. Gray arrows indicate partially characterized signaling pathways. AC, adenylate cyclase.

a close relation between thyroid follicular and endothelial cells, in which TSH-independent mechanisms may stimulate thyroid cell metabolism to promote angiogenesis.

Physiological mediators of NO activity involve canonical cGMP/cGK signaling and the noncanonical pathway in which NO regulates protein function through S-nitrosylation (17). In dog thyroid slices, Ca<sup>2+</sup> signaling activation significantly increased NOS-mediated cGMP production (11). Similarly, NO donors induced dose-dependent cGMP production in thyroid cells (13). Bocanera et al (15) reported acute repression of I<sup>-</sup> uptake in response to cGK activators in calf thyroid primary cultures. In agreement with this, Bazzara et al (13) demonstrated that long-term incubation with NO donors reduced I<sup>-</sup> uptake involving cGK signaling activation in rat thyrocytes. Conversely, although blockage of NOS activity reversed cytokine-abrogated cell proliferation, NO donors, but not cGMP analogs, inhibited cell growth, suggesting that NO also exerts cGMP-independent inhibitory effects on human thyrocytes (45). Gérard et al (42) postulated that NO may control I<sup>-</sup> organization through an S-nitrosylation-dependent process involving proteasome-mediated TPO and thyroid oxidase degradation. Here, we propose a novel cGMP-independent mechanism for NO-induced inhibition of NIS-mediated I<sup>-</sup> uptake in rat thyroid cells involving transcrip-

reduction in vasculature during goiter formation. Subsequently, Colin et al (9) observed an increase in NOS III protein in samples from hyperthyroid patients, whereas NOS III was barely detectable in hypothyroid patients. In accordance with these findings, Gérard et al (12) demonstrated that NOS III expression is restricted to active thyroid follicles, thus suggesting that paracrine NO-promoted microvascular blood flow is required to sustain hormone production. Recently, Craps et al (44) demonstrated that I<sup>-</sup> deficiency-induced thyroidal blood flow relies on increased NOS III-mediated NO production. These observations are consistent with the existence of

tional repression of NF-κB-activated NIS gene expression in response to stimulation by TSH. Our data indicate that NO donors repress TSH-induced NIS gene expression by reducing the transcriptional activity of the NF-κB subunit p65. S-nitrosylation of p65 at Cys-38 impairs its binding to DNA and thus suppresses p65-dependent gene expression (20). Consistent with this, overexpression of the nonnitrosylatable C38S p65 mutant abrogated NO-repressed NIS promoter activity. Moreover, we detected p65 S-nitrosylation in response to NO donor treatment using the biotin-switch technique. Taken together, these findings indicate that p65 S-nitrosylation plays a previ-

ously undiscovered role in regulating TSH-stimulated NIS transcriptional expression.

Mounting evidence supports a role for S-nitrosylation as a major NO-dependent posttranslational mechanism in the direct regulation of protein function (17). In recent years, several studies have reported that S-nitrosylation participates in regulating physiological hormone-stimulated cellular processes. In human umbilical vein endothelial cells,  $17\beta$ -estradiol stimulates protein S-nitrosylation by increasing NOS III-generated NO levels (46). S-nitroso-proteome analysis has suggested that S-nitrosylation regulates several endothelial functions, including mitochondrial functions and cellular cytoskeleton remodeling (46–48). In addition, NO-induced S-nitrosylation of the  $\alpha$ -isoform of the estrogen receptor at  $Zn^{2+}$ -coordinating cysteine residues in the 2 major DNA-binding Zn-finger domains inhibits the binding of the receptor to DNA, repressing the genomic actions of estrogen (49). In pancreatic  $\beta$ -cells, insulin regulates the activity of glucokinase by modulating its association with insulin-secreting granules. Insulin-stimulated NO production leads to the S-nitrosylation of glucokinase and its dissociation from secretory granules, thus reducing the cellular activity of glucokinase, because secretory granules function as a storage pool for glucokinase (50). Moreover, in obesity, insulin resistance has been associated with increased S-nitrosylation of proteins involved in the insulin signaling cascade (51). Increased S-nitrosylation has been observed in obesity-associated adipose tissue and suggested to contribute to adipocyte resistance to insulin. In adipocytes, S-nitrosylation targets the antilipolytic action of insulin, leading to the dysregulated lipolysis observed in the pathogenesis of obesity-associated metabolic dysfunction (52).

Colin et al (9) reported increased expression of NOS III in thyroid follicular cells from patients with Graves' disease and autonomous toxic adenomas harboring activating TSHR mutations. Previous results from our group have revealed the ability of TSH-stimulated endogenously produced NO to inhibit thyroid cell function and differentiation. Using nonselective NOS inhibitors, we have shown that inhibition of NOS activity increases TSH-stimulated thyroid differentiation markers and cell proliferation, revealing that there may be an inhibitory autocrine pathway that modulates TSH-stimulated thyroid cell function (16). Accumulated evidence led us to hypothesize that TSH-stimulated NF- $\kappa$ B-mediated gene expression might be counterbalanced by TSH-dependent stimulation of NOS III-produced NO, leading to inhibition of NF- $\kappa$ B transcriptional activity through S-nitrosylation. Accordingly, Kelleher et al (20) suggested a counter-regulatory mechanism by which NF- $\kappa$ B-induced NOS II activity in response to proinflammatory cytokines down-regulated

NF- $\kappa$ B-dependent gene expression through S-nitrosylation in macrophages, thus providing a feedback loop limiting inflammation.

Pathological conditions are often associated with NOS overexpression and unregulated NO production, resulting in inappropriate S-nitrosylation-regulated cellular processes that may contribute to pathological phenotypes (53, 54). Although NO and other oxygen radicals have been shown to be important factors related to tumorigenesis (55, 56), the role of NO in thyroid carcinogenesis remains unclear. NOS overexpression has been demonstrated in papillary thyroid carcinoma and autoimmune thyroid disease (57). Consistent with this, Nakamura et al (58) reported increased nitrotyrosine-modified protein levels, an indicator of NO overproduction, in samples from primary papillary thyroid tumors. In addition, van den Hove et al (43) have proposed that NO mediates cytokine-induced cytotoxic effects and functional injuries to follicular cells in autoimmune thyroiditis. In thyroid cancer, NOS II-generated NO-mediated S-nitrosylation and the subsequent nuclear translocation of glyceraldehyde-3-phosphate dehydrogenase might be implicated in TRAIL-mediated anaplastic thyroid cancer cell death (59). In addition, NO-mediated long-term inhibition of thyroid hormonogenesis could shed light on human thyroid pathologies associated with chronic NO production.

The elucidation of the underlying mechanism controlling NIS expression in the thyroid may have important implications not only for understanding the pathways regulating thyroid hormone biosynthesis but also for the development of novel strategies for improving NIS-mediated radioiodide therapy for treating thyroid cancer (60). Here, we have demonstrated that exogenous NO-induced p65 S-nitrosylation represses TSH-stimulated NIS transcriptional expression, thus reducing NIS-mediated  $I^-$  uptake in rat thyrocytes. Future studies of S-nitrosylation in radioiodide-refractory thyroid tumors may provide novel therapeutic strategies for increasing NIS expression, thereby making possible more effective radiotherapy regimens.

## Acknowledgments

We thank Dr Nancy Carrasco (Yale University School of Medicine, New Haven, CT) for plasmid encoding HA-tagged NIS, affinity-purified anti-NIS antibody, and extensive critical review of the manuscript; Dr Pilar Santisteban (Instituto de Investigaciones Biomédicas Alberto Sols, Madrid, Spain) and Dr Roberto Di Lauro (Università degli Studi di Napoli Federico II, Naples, Italy) for kindly providing NIS-promoter constructs and Dr Di-

AQ: 21

AQ:22–23

etmar Spengler (Max Planck Institute of Psychiatry, Munich, Germany) for supplying the reporter 5xCRE-Luc; and Dr Daemyung Jue (Catholic University of Korea, Seoul, Republic of Korea) for providing wild-type p65 and C38S p65 expression vectors and the members of our laboratory for helpful technical assistance and critical insights.

Address all correspondence and requests for reprints to: Dr Ana María Masini-Repiso, Centro de Investigaciones en Bioquímica Clínica e Inmunología, Consejo Nacional de Investigaciones Científicas y Técnicas, Departamento de Bioquímica Clínica, Facultad de Ciencias Químicas, Universidad Nacional de Córdoba. Haya de la Torre y Medina Allende, 5000 Córdoba, Argentina. E-mail: amasini@fcq.unc.edu.ar.

This work was supported by grants from the Latin American Thyroid Society (J.P.N.), the Agencia Nacional de Promoción Científica y Tecnológica, the Consejo Nacional de Investigaciones Científicas y Técnicas, the Ministerio de Ciencia y Tecnología de la Provincia de Córdoba, and the Secretaría de Ciencia y Tecnología de la Universidad Nacional de Córdoba (C.G.P. and A.M.M.-R.).

Disclosure Summary: The authors have nothing to disclose.

## References

- Serrano-Nascimento C, da Silva Teixeira S, et al. The acute inhibitory effect of iodide excess on sodium/iodide symporter expression and activity involves the PI3K/Akt signaling pathway. *Endocrinology*. 2014;155:1145–1156.
- Nicola JP, Carrasco N. The Na<sup>+</sup>/I<sup>-</sup> symporter (NIS) and thyroid hormone biosynthesis. In: Ulloa-Aguirre A, Conn PM, eds. *Cellular Endocrinology in Health and Disease*. San Diego, CA: Academic Press; 2014:65–83.
- Kogai T, Endo T, Saito T, Miyazaki A, Kawaguchi A, Onaya T. Regulation by thyroid-stimulating hormone of sodium/iodide symporter gene expression and protein levels in FRTL-5 cells. *Endocrinology*. 1997;138:2227–2232.
- Ohno M, Zannini M, Levy O, Carrasco N, Di Lauro R. The paired-domain transcription factor Pax8 binds to the upstream enhancer of the rat sodium/iodide symporter gene and participates in both thyroid-specific and cyclic-AMP-dependent transcription. *Mol Cell Biol*. 1999;19:2051–2060.
- Chun JT, Di Dato V, D'Andrea B, Zannini M, Di Lauro R. The CRE-like element inside the 5'-upstream region of the rat sodium/iodide symporter gene interacts with diverse classes of b-Zip molecules that regulate transcriptional activities through strong synergy with Pax-8. *Mol Endocrinol*. 2004;18:2817–2829.
- Nicola JP, Nazar M, Mascanfroni ID, Pellizas CG, Masini-Repiso AM. NF-κB p65 subunit mediates lipopolysaccharide-induced Na(+)/I(-) symporter gene expression by involving functional interaction with the paired domain transcription factor Pax8. *Mol Endocrinol*. 2010;24:1846–1862.
- Bogdan C. Nitric oxide and the immune response. *Nat Immunol*. 2001;2:907–916.
- Fukumura D, Kashiwagi S, Jain RK. The role of nitric oxide in tumour progression. *Nat Rev Cancer*. 2006;6:521–534.
- Colin IM, Kopp P, Zbären J, Häberli A, Grizzle WE, Jameson JL. Expression of nitric oxide synthase III in human thyroid follicular cells: evidence for increased expression in hyperthyroidism. *Eur J Endocrinol*. 1997;136:649–655.
- Colin IM, Nava E, Toussaint D, et al. Expression of nitric oxide synthase isoforms in the thyroid gland: evidence for a role of nitric oxide in vascular control during goiter formation. *Endocrinology*. 1995;136:5283–5290.
- Esteves RZ, van Sande J, Dumont JE. Nitric oxide as a signal in thyroid. *Mol Cell Endocrinol*. 1992;90:R1–R3.
- Gérard AC, Many MC, Daumerie C, et al. Structural changes in the angiofollicular units between active and hypofunctioning follicles align with differences in the epithelial expression of newly discovered proteins involved in iodine transport and organification. *J Clin Endocrinol Metab*. 2002;87:1291–1299.
- Bazzara LG, Vélez ML, Costamagna ME, et al. Nitric oxide/cGMP signaling inhibits TSH-stimulated iodide uptake and expression of thyroid peroxidase and thyroglobulin mRNA in FRTL-5 thyroid cells. *Thyroid*. 2007;17:717–727.
- Costamagna ME, Cabanillas AM, Coleoni AH, Pellizas CG, Masini-Repiso AM. Nitric oxide donors inhibit iodide transport and organification and induce morphological changes in cultured bovine thyroid cells. *Thyroid*. 1998;8:1127–1135.
- Bocanera LV, Krawiec L, Silberschmidt D, et al. Role of cyclic 3',5' guanosine monophosphate and nitric oxide in the regulation of iodide uptake in calf thyroid cells. *J Endocrinol*. 1997;155:451–457.
- Fozzatti L, Vélez ML, Lucero AM, et al. Endogenous thyrocyte-produced nitric oxide inhibits iodide uptake and thyroid-specific gene expression in FRTL-5 thyroid cells. *J Endocrinol*. 2007;192:627–637.
- Martínez-Ruiz A, Cadenas S, Lamas S. Nitric oxide signaling: classical, less classical, and nonclassical mechanisms. *Free Radic Biol Med*. 2011;51:17–29.
- Sha Y, Marshall HE. S-nitrosylation in the regulation of gene transcription. *Biochim Biophys Acta*. 2012;1820:701–711.
- Marshall HE, Hess DT, Stamler JS. S-nitrosylation: physiological regulation of NF-κB. *Proc Natl Acad Sci USA*. 2004;101:8841–8842.
- Kelleher ZT, Matsumoto A, Stamler JS, Marshall HE. NOS2 regulation of NF-κB by S-nitrosylation of p65. *J Biol Chem*. 2007;282:30667–30672.
- Costamagna E, García B, Santisteban P. The functional interaction between the paired domain transcription factor Pax8 and Smad3 is involved in transforming growth factor-β repression of the sodium/iodide symporter gene. *J Biol Chem*. 2004;279:3439–3446.
- Baratta MG, Porreca I, Di Lauro R. Oncogenic ras blocks the cAMP pathway and dedifferentiates thyroid cells via an impairment of pax8 transcriptional activity. *Mol Endocrinol*. 2009;23:838–848.
- Spengler D, Rupprecht R, Van LP, Holsboer F. Identification and characterization of a 3',5'-cyclic adenosine monophosphate-responsive element in the human corticotropin-releasing hormone gene promoter. *Mol Endocrinol*. 1992;6:1931–1941.
- Espinosa L, Santos S, Inglés-Esteve J, Muñoz-Canoves P, Bigas A. p65-NFκB synergizes with Notch to activate transcription by triggering cytoplasmic translocation of the nuclear receptor corepressor N-CoR. *J Cell Sci*. 2002;115:1295–1303.
- Ha KH, Byun MS, Choi J, Jeong J, Lee KJ, Jue DM. N-tosyl-L-phenylalanine chloromethyl ketone inhibits NF-κB activation by blocking specific cysteine residues of IκB kinase β and p65/RelA. *Biochemistry*. 2009;48:7271–7278.
- Paroder-Belenitsky M, Maestas MJ, Dohán O, et al. Mechanism of anion selectivity and stoichiometry of the Na<sup>+</sup>/I<sup>-</sup> symporter (NIS). *Proc Natl Acad Sci USA*. 2011;108:17933–17938.
- Purtell K, Paroder-Belenitsky M, Reyna-Neyra A, et al. The KCNQ1-KCNE2 K<sup>+</sup> channel is required for adequate thyroid I<sup>-</sup> uptake. *FASEB J*. 2012;26:3252–3259.
- Nicola JP, Carrasco N, Amzel LM. Physiological sodium concentrations enhance the iodide affinity of the Na(+)/I(-) symporter. *Nat Commun*. 2014;5:3948.
- Nazar M, Nicola JP, Vélez ML, Pellizas CG, Masini-Repiso AM. Thyroid peroxidase gene expression is induced by lipopolysaccha-

- ride involving nuclear factor (NF)- $\kappa$ B p65 subunit. *Endocrinology*. 2012;153:6114–6125.
30. Nicola JP, Reyna-Neyra A, Carrasco N, Masini-Repiso AM. Dietary iodide controls its own absorption through post-transcriptional regulation of the intestinal Na<sup>+</sup>/I<sup>-</sup> symporter. *J Physiol*. 2012;590:6013–6026.
  31. Romero JM, Bizzozero OA. Intracellular glutathione mediates the denitrosylation of protein nitrosothiols in the rat spinal cord. *J Neurosci Res*. 2009;87:701–709.
  32. Riedel C, Levy O, Carrasco N. Post-transcriptional regulation of the sodium/iodide symporter by thyrotropin. *J Biol Chem*. 2001;276:21458–21463.
  33. Weiss SJ, Philp NJ, Ambesi-Impiomato FS, Grollman EF. Thyrotropin-stimulated iodide transport mediated by adenosine 3',5'-monophosphate and dependent on protein synthesis. *Endocrinology*. 1984;114:1099–1107.
  34. Antonica F, Kasprzyk DF, Opitz R, et al. Generation of functional thyroid from embryonic stem cells. *Nature*. 2012;491:66–71.
  35. Morshed SA, Latif R, Davies TF. Characterization of thyrotropin receptor antibody-induced signaling cascades. *Endocrinology*. 2009;150:519–529.
  36. Cao X, Kambe F, Seo H. Requirement of thyrotropin-dependent complex formation of protein kinase A catalytic subunit with inhibitor of  $\kappa$ B proteins for activation of p65 nuclear factor- $\kappa$ B by tumor necrosis factor- $\alpha$ . *Endocrinology*. 2005;146:1999–2005.
  37. Vallabhapurapu S, Karin M. Regulation and function of NF- $\kappa$ B transcription factors in the immune system. *Annu Rev Immunol*. 2009;27:693–733.
  38. Hayden MS, Ghosh S. Shared principles in NF- $\kappa$ B signaling. *Cell*. 2008;132:344–362.
  39. Ruland J. Return to homeostasis: downregulation of NF- $\kappa$ B responses. *Nat Immunol*. 2011;12:709–714.
  40. Forrester MT, Foster MW, Benhar M, Stamler JS. Detection of protein S-nitrosylation with the biotin-switch technique. *Free Radic Biol Med*. 2009;46:119–126.
  41. Kasai K, Hattori Y, Nakanishi N, et al. Regulation of inducible nitric oxide production by cytokines in human thyrocytes in culture. *Endocrinology*. 1995;136:4261–4270.
  42. Gérard AC, Boucquey M, van den Hove MF, Colin IM. Expression of TPO and ThOXs in human thyrocytes is downregulated by IL-1 $\alpha$ /IFN- $\gamma$ , an effect partially mediated by nitric oxide. *Am J Physiol Endocrinol Metab*. 2006;291:E242–E253.
  43. van den Hove MF, Stoenoiu MS, Croizet K, et al. Nitric oxide is involved in interleukin-1 $\alpha$ -induced cytotoxicity in polarised human thyrocytes. *J Endocrinol*. 2002;173:177–185.
  44. Craps J, Wilvers C, Joris V, et al. Involvement of nitric oxide in iodine deficiency-induced microvascular remodeling in the thyroid gland: role of nitric oxide synthase 3 and ryanodine receptors. *Endocrinology*. 2015;156:707–720.
  45. Motohashi S, Kasai K, Banba N, Hattori Y, Shimoda S. Nitric oxide inhibits cell growth in cultured human thyrocytes. *Life Sci*. 1996;59:PL227–234.
  46. Zhang HH, Feng L, Livnat I, et al. Estradiol-17 $\beta$  stimulates specific receptor and endogenous nitric oxide-dependent dynamic endothelial protein S-nitrosylation: analysis of endothelial nitrosyl-proteome. *Endocrinology*. 2010;151:3874–3887.
  47. Satohisa S, Zhang HH, Feng L, Yang YY, Huang L, Chen DB. Endogenous NO upon estradiol-17 $\beta$  stimulation and NO donor differentially regulate mitochondrial S-nitrosylation in endothelial cells. *Endocrinology*. 2014;155:3005–3016.
  48. Zhang HH, Lechuga TJ, Tith T, Wang W, Wing DA, Chen DB. S-nitrosylation of cofilin-1 mediates estradiol-17 $\beta$ -stimulated endothelial cytoskeleton remodeling. *Mol Endocrinol*. 2015;29:434–444.
  49. Garbán HJ, Márquez-Garbán DC, Pietras RJ, Ignarro LJ. Rapid nitric oxide-mediated S-nitrosylation of estrogen receptor: regulation of estrogen-dependent gene transcription. *Proc Natl Acad Sci USA*. 2005;102:2632–2636.
  50. Markwardt ML, Nkobena A, Ding SY, Rizzo MA. Association with nitric oxide synthase on insulin secretory granules regulates glucokinase protein levels. *Mol Endocrinol*. 2012;26:1617–1629.
  51. Carvalho-Filho MA, Ueno M, Hirabara SM, et al. S-nitrosation of the insulin receptor, insulin receptor substrate 1, and protein kinase B/Akt: a novel mechanism of insulin resistance. *Diabetes*. 2005;54:959–967.
  52. Ovadia H, Haim Y, Nov O, et al. Increased adipocyte S-nitrosylation targets anti-lipolytic action of insulin: relevance to adipose tissue dysfunction in obesity. *J Biol Chem*. 2011;286:30433–30443.
  53. Wang Z. Protein S-nitrosylation and cancer. *Cancer Lett*. 2012;320:123–129.
  54. Foster MW, Hess DT, Stamler JS. Protein S-nitrosylation in health and disease: a current perspective. *Trends Mol Med*. 2009;15:391–404.
  55. Ying L, Hofseth LJ. An emerging role for endothelial nitric oxide synthase in chronic inflammation and cancer. *Cancer Res*. 2007;67:1407–1410.
  56. Hussain SP, Hofseth LJ, Harris CC. Radical causes of cancer. *Nat Rev Cancer*. 2003;3:276–285.
  57. Donckier JE, Michel L, Delos M, Havaux X, Van Beneden R. Interrelated overexpression of endothelial and inducible nitric oxide synthases, endothelin-1 and angiogenic factors in human papillary thyroid carcinoma. *Clin Endocrinol (Oxf)*. 2006;64:703–710.
  58. Nakamura Y, Yasuoka H, Zuo H, et al. Nitric oxide in papillary thyroid carcinoma: induction of vascular endothelial growth factor D and correlation with lymph node metastasis. *J Clin Endocrinol Metab*. 2006;91:1582–1585.
  59. Du ZX, Wang HQ, Zhang HY, Gao DX. Involvement of glyceraldehyde-3-phosphate dehydrogenase in tumor necrosis factor-related apoptosis-inducing ligand-mediated death of thyroid cancer cells. *Endocrinology*. 2007;148:4352–4361.
  60. Riesco-Eizaguirre G, Santisteban P. A perspective view of sodium iodide symporter research and its clinical implications. *Eur J Endocrinol*. 2006;155:495–512.